



HAL
open science

Equilibrium surface complexation modeling with metastable natural colloids: the key to predict the oxidation state distribution of trace elements?

Rémi Marsac, Charlotte Catrouillet, Mathieu Pédrot, Marc F Benedetti, Aline Dia, Eric D van Hullebusch, Mélanie Davranche, Yann Sivry, Anne-Catherine Pierson-Wickmann, Mickael Tharaud, et al.

► To cite this version:

Rémi Marsac, Charlotte Catrouillet, Mathieu Pédrot, Marc F Benedetti, Aline Dia, et al.. Equilibrium surface complexation modeling with metastable natural colloids: the key to predict the oxidation state distribution of trace elements?. *Current Opinion in Colloid & Interface Science*, 2024, 72, pp.101820. 10.1016/j.cocis.2024.101820 . insu-04608979

HAL Id: insu-04608979

<https://insu.hal.science/insu-04608979v1>

Submitted on 12 Jun 2024

HAL is a multi-disciplinary open access archive for the deposit and dissemination of scientific research documents, whether they are published or not. The documents may come from teaching and research institutions in France or abroad, or from public or private research centers.

L'archive ouverte pluridisciplinaire **HAL**, est destinée au dépôt et à la diffusion de documents scientifiques de niveau recherche, publiés ou non, émanant des établissements d'enseignement et de recherche français ou étrangers, des laboratoires publics ou privés.



Distributed under a Creative Commons Attribution 4.0 International License

Journal Pre-proof

Equilibrium surface complexation modeling with metastable natural colloids: the key to predict the oxidation state distribution of trace elements?

Rémi Marsac, Charlotte Catrouillet, Mathieu Pédrot, Marc F. Benedetti, Aline Dia, Eric D. van Hullebusch, Mélanie Davranche, Yann Sivry, Anne-Catherine Pierson-Wickmann, Mickael Tharaud, Frank Heberling

PII: S1359-0294(24)00038-4

DOI: <https://doi.org/10.1016/j.cocis.2024.101820>

Reference: COCIS 101820

To appear in: *Current Opinion in Colloid & Interface Science*

Received Date: 29 October 2023

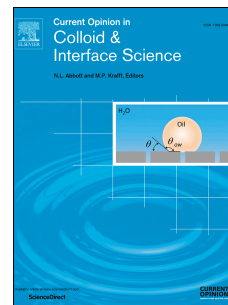
Revised Date: 18 April 2024

Accepted Date: 4 June 2024

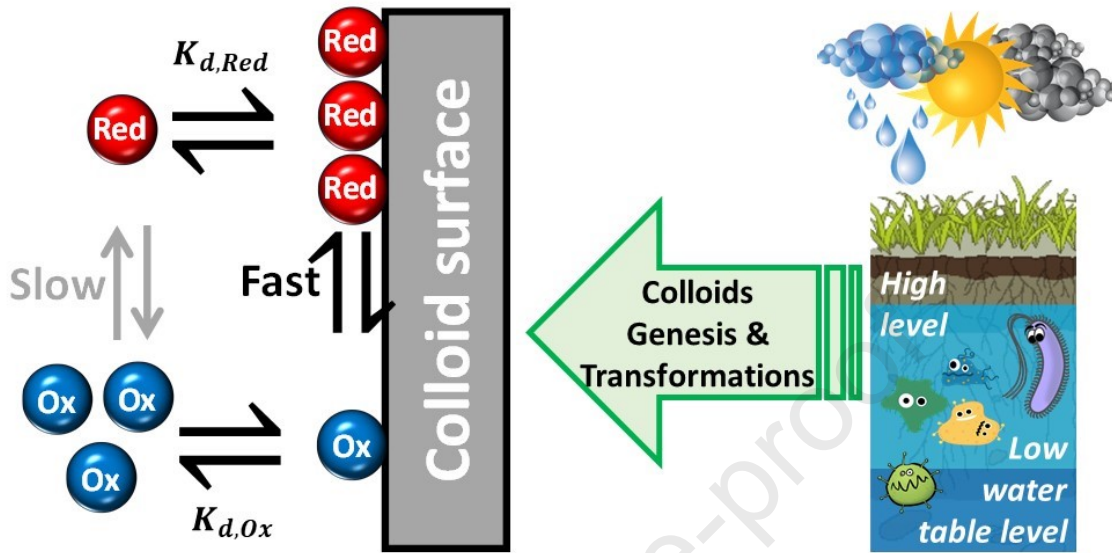
Please cite this article as: Marsac R, Catrouillet C, Pédrot M, Benedetti MF, Dia A, van Hullebusch ED, Davranche M, Sivry Y, Pierson-Wickmann A-C, Tharaud M, Heberling F, Equilibrium surface complexation modeling with metastable natural colloids: the key to predict the oxidation state distribution of trace elements?, *Current Opinion in Colloid & Interface Science*, <https://doi.org/10.1016/j.cocis.2024.101820>.

This is a PDF file of an article that has undergone enhancements after acceptance, such as the addition of a cover page and metadata, and formatting for readability, but it is not yet the definitive version of record. This version will undergo additional copyediting, typesetting and review before it is published in its final form, but we are providing this version to give early visibility of the article. Please note that, during the production process, errors may be discovered which could affect the content, and all legal disclaimers that apply to the journal pertain.

© 2024 The Author(s). Published by Elsevier Ltd.



$$\frac{[Ox]_{aq}}{[Red]_{aq}} = \frac{[Ox]_{surf}}{[Red]_{surf}} \times \frac{K_{d,Ox}}{K_{d,Red}} = f(\text{Hydro/bio/pedological and climatic conditions})$$



1 **Equilibrium surface complexation modeling with metastable**
2 **natural colloids: the key to predict the oxidation state**
3 **distribution of trace elements?**
4

5 Rémi Marsac^{1,2*}, Charlotte Catrouillet¹, Mathieu Pédrot², Marc F. Benedetti¹, Aline Dia², Eric
6 D. van Hullebusch¹, Mélanie Davranche², Yann Sivry¹, Anne-Catherine Pierson-Wickmann²,
7 Mickael Tharaud¹, Frank Heberling³

8 ¹ Université Paris Cité, Institut de Physique du Globe de Paris, CNRS, F-75005 Paris, France

9 ² Univ Rennes, CNRS, Géosciences Rennes - UMR 6118, F-35000, Rennes, France

10 ³ Institute for Nuclear Waste Disposal (INE), Karlsruhe Institute of Technology (KIT), P.O.
11 Box 3640, D-76021 Karlsruhe, Germany

12 * Corresponding author: remi.marsac@cnrs.fr
13
14

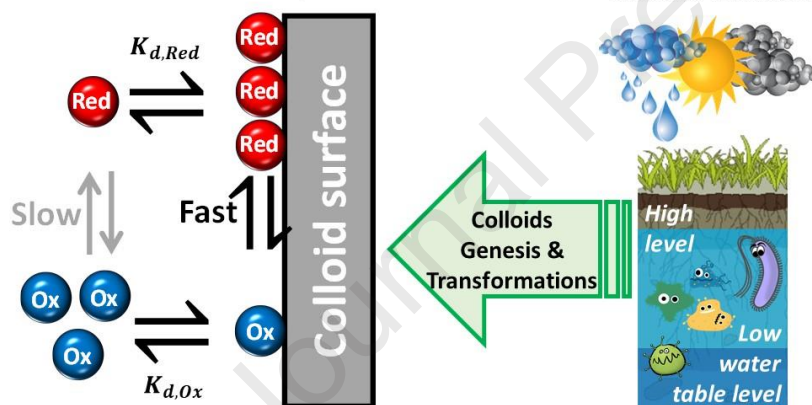
15 **Abstract**

16 Predicting the behavior and fate of redox-sensitive trace elements (TEs; e.g., As, U, Cu, Cr) in
 17 natural systems is challenging. Colloids have been reported to control TEs speciation and
 18 catalyze TEs redox reactions in many environments. We hypothesize that the lack of accurate
 19 thermodynamic models that account for the role of colloids in TEs speciation explains our
 20 inability to predict their redox state distribution in the environment. The slow evolution of the
 21 colloidal compartment in response to prevailing bio/hydro/pedo/climatological conditions
 22 needs to be decoupled from the fast TEs redox reactions promoted by colloidal surfaces.
 23 Further progress is hampered by experimental and theoretical challenges associated with
 24 capturing the extreme physical and chemical heterogeneity of colloids, their metastable
 25 structures, and their dynamic transformation behavior.

26

27 **Graphical abstract**

$$\frac{[Ox]_{aq}}{[Red]_{aq}} = \frac{[Ox]_{surf}}{[Red]_{surf}} \times \frac{K_{d,Ox}}{K_{d,Red}} = f(\text{Hydro/bio/pedological and climatic conditions})$$



28

29 1 Introduction

30 Redox reactions play a key role on the biogeochemical cycles of many elements in the
31 environment. These include C, with effects on climate change or soil quality, and nutrients of
32 paramount importance for living organisms such as N or Fe. It also applies for many trace
33 elements (TEs), from metals (e.g., Cr, Cu, Ce), radionuclides (e.g., U, Pu, Tc), to metalloids or
34 non-metals (e.g., As, Sb, Se) displaying negative effects on the environment and/or human
35 health. For instance, As, Cr and Cu are generally considered as toxic (at least above certain
36 concentrations), but As(III), Cr(VI), and Cu(I) are much more toxic for living organisms
37 compared to As(V), Cr(III) and Cu(II), respectively [1–3]. Actinides and Tc in their tetravalent
38 state (U/Np/Pu/Tc(IV)) exhibit very low solubilities and may be considered much less mobile
39 and bioavailable than the oxidized forms (i.e. U(VI)/Np/Pu(V)/Tc(VII)) [4,5]. Therefore,
40 predicting the redox state and speciation of TEs is crucial to understand their behavior and
41 fate in the environment, for risk assessments for health, ecosystems and development of
42 remediation strategies.

43 Thermodynamic models are thought to provide inaccurate predictions in the environment [6–
44 8]. Indeed, as far as thermodynamics is concerned, many important redox reactions should
45 proceed in the environment (involving redox couples e.g. CO₂/organic C, Fe(OH)_{3(s)}/Fe²⁺,
46 O₂/H₂O, NO₃⁻/NH₄⁺/N₂, SO₄²⁻/HS⁻), but, in reality many compounds persist due to strong kinetic
47 constrains [1,3,7,9]. In addition, under the influence of combined effects of
48 bio/hydro/pedo/climatological conditions [9,10], large fluctuations or gradients of pH and
49 redox potential (E_H) might occur over too short time scales in the environment, which may
50 prohibit the attainment of thermodynamic equilibria, and instead cause the formation of
51 metastable compounds. These include for example amorphous nano-phases/colloids such as
52 clay minerals, metal oxides or sulfides, and organic colloids with a large heterogeneity of
53 reactive sites, and thus a broad variety of redox potentials [9,11–13] with varying electron
54 donating/accepting capacities [14]. In addition, coupling between the biogeochemical cycles
55 of elements must be considered, such as the impact of organo-mineral associations on C
56 preservation in soils or the role of Fe in the C and N redox cycles [15–17]. In view of the
57 extreme complexity of natural systems, characterized by a high degree of chemical and
58 physical heterogeneity, with processes occurring over various spatial and temporal scales, and
59 the lack of numerical models to take this complexity into account, predicting the redox state

60 distribution of TEs, whose biogeochemical cycle is dictated by major elements (e.g.
61 C/S/N/Fe/Mn/Al/Si), seems currently not achievable. Therefore, new ideas and conceptual
62 frameworks are urgently needed to better understand the driving parameters of TEs dynamics
63 and trajectories in natural environments, and to provide efficient predictive tools for
64 understanding and constraining their behavior and fate.

65 Colloids are ubiquitous in aquatic environmental systems and, with their small size (typically
66 ranging from a few nanometers to a few micrometers), large and highly reactive surface
67 towards TEs, they largely control the speciation of TEs. For instance, they can transport TEs
68 over long distances in groundwaters [18], from soils to water bodies, in tropical [19,20],
69 temperate [21] and subarctic [22,23] regions, or from continents to oceans, because colloid
70 flocculation in estuaries traps many TEs in sediments [24]. Accordingly, the impact of colloids
71 on the redox state distribution of TEs must correctly be considered in geochemical speciation
72 models. Like engineered nanoparticles, natural colloids can catalyze chemical reactions,
73 including redox transformations. Indeed, there is plethora of scientific articles reporting the
74 catalytic activity of nanoparticles and colloids towards redox transformation of TEs in
75 environmentally relevant conditions [3,25–28]. Colloids may even be compared to enzymes
76 for their catalytic activities [29,30], and have sometimes been shown more efficient than biotic
77 processes [31]. The fact that TEs redox reactions at colloid-water interface proceed rapidly
78 might encourage the use of equilibrium speciation modelling, but this rarely the case. Only
79 few studies, often dedicated to actinide, successfully used equilibrium modelling to predict
80 TEs oxidation state distribution [26,32–38].

81 The limitations of equilibrium speciation models for predicting the oxidation state distribution
82 (or "redox speciation") of TEs are discussed here, as well as recent results that support a
83 broader use of these tools to unravel some important aspects hidden behind the complexity
84 of natural environments. The fact that colloids are metastable nanophases, whose
85 composition and structure is impacted by combined effects of bio/hydro/pedo/climatological
86 conditions, suggests that equilibrium models are of little help as far as colloids are concerned.
87 However, as pointed out by Alexandra Navrotsky: "*we ourselves are metastable with respect*
88 *to CO₂, H₂O, and a small pile of ash, but that does not matter for most of our lives*" [39]. In
89 other words, over a relevant time scale where metastable phases persist, their
90 thermodynamic properties can be studied. For instance, equilibrium calculations are the most
91 relevant to predict radionuclide migration in the context of nuclear waste disposal in deep

92 geological environments, because reaction rates (time scales from seconds to years) are low
 93 compared to the half-life of relevant radionuclides (up to thousands or millions of years) [4,5].
 94 Recent thermodynamic investigations of metastable phases provide evidence that many of
 95 the behaviors that we have previously ascribed to kinetics are, in fact, thermodynamically
 96 driven, such as the polymorphism of metal oxides, dehydration and redox reactions [40,41].
 97 Under kinetic constraints, thermodynamics may still guide the processes, such as in the case
 98 of the redox reactions involving Fe-oxides [27,28,42]. More generally, thermodynamics allows
 99 us to judge which reactions are possible or in which direction they may be expected to
 100 proceed. Because thermodynamics clearly point to the oxidation of colloidal organic matter
 101 to CO₂ in the presence of O₂, we can claim that this system is constrained by kinetics. The same
 102 reasoning can be applied to any mixture of a strong reductant and an oxidized form of a TE (or
 103 the contrary). However, this may not be so straightforward in all natural systems where TEs
 104 can experience a wide range of redox conditions and where TEs are indeed intimately
 105 associated with colloids. Accordingly, the appropriate description of the influence of colloids
 106 and surfaces on the redox speciation of TEs is presently discussed as an important key for a
 107 holistic understanding and modeling of the fate and behavior of TEs in environmental systems.

108

109 **2 Reasons for the inefficiency of previous equilibrium modeling approaches**

110 The distribution of the redox states of an element should be predicted using the Nernst
 111 equation as follows:

112

$$113 \quad E_H = E_{Ox/Red}^0 + \frac{RT}{nF} \log \left(\frac{[Ox] \times \gamma_{Ox}}{[Red] \times \gamma_{Red}} \right) + \frac{m}{n} pH \quad (1)$$

114

115 Where E_H is the redox potential, T is absolute temperature, F is the Faraday constant and R is
 116 the gas constant, "Ox" and "Red" are oxidized and reduced species of an element, γ_{Ox} and γ_{Red}
 117 are their respective activity coefficients, brackets denote concentrations, $E_{Ox/Red}^0$ is the
 118 standard redox potential of the Ox/Red couple, n and m are the number of electrons and
 119 protons, respectively, involved in the redox reaction that can be written as follows:

120



122

123 Equation 1 relies on concentrations of chemical species (e.g. $[Fe^{2+}]$ and $[Fe^{3+}]$), which often
124 differ from their total concentrations ($[Fe(II)]$ and $[Fe(III)]$, keeping the Fe example)) that are
125 detected in natural samples using spectrophotometry, mass spectrometry or electrochemistry
126 when the instruments are calibrated against total element concentration. The relationship
127 between total and species concentrations of an element under a given oxidation state can be
128 written, using the example of Fe(II), as follows:

129

$$130 \quad [Fe(II)] = [Fe^{2+}] + \sum_i [FeL_i] \quad (3)$$

131

132 Where L_i is a i -th ligand in solution (including, e.g., OH^- , Cl^- , organic acids), which can form
133 complexes with Fe^{2+} . For the sake of simplicity, equation 3 does not show other Fe:L
134 stoichiometries than 1:1 and it omits charges of the complexes. Nevertheless, it shows that
135 knowing the Fe speciation in the sample precisely is a mandatory prerequisite to use the
136 Nernst equation. This includes concentrations of all ligands and the corresponding
137 complexation reactions and constants with both Fe^{2+} and Fe^{3+} . Popular geochemical speciation
138 software (e.g. PHREEQC [43], Visual Minteq [44]), include extensive aqueous chemical
139 reaction databases for this purpose.

140 As discrepancies between measurements and equilibrium calculations are common [3,6–8],
141 the Nernst equation is very often used to conclude that the system has not reached
142 equilibrium. Alternatively, failure in the use of the Nernst equation might be attributed to the
143 extreme sensitivity of the calculations to uncertainties related, for instance, to E_H
144 determination, which is subjected to numerous limitations and artifacts [6,7,45], or the
145 accuracy of the chemical reaction database. However, the fact that filtered natural samples
146 (e.g. $<0.2\mu m$) are no more than colloid suspensions [18–23,46] is a major limitation that
147 should be considered. In principle, such nano-phases are solid particles that should be ideally
148 removed from the solution by filtration however this is hardly achieved, unless much more
149 rigorous separation procedures are applied. For Fe, it is well known that the presence of
150 (hydr)oxide nanophase must be taken into account to predict its solubility and redox
151 speciation [46]. Similarly, application of the Nernst equation to predict TE redox speciation
152 should consider adsorption processes (e.g. cation exchange, surface complexation) occurring
153 at the colloids-water interfaces, but this is generally overlooked in geochemical speciation
154 calculations.

155 3 Recently developed approaches to model the redox speciation of TEs on 156 the surface of particles and colloids

157 3.1 Thermodynamics at the colloid-water interface

158 For many redox-sensitive TEs (e.g. V, Cr, Mn, Cu, As, Se, Mo, Tc, Sb, Ce, actinides), whose
159 speciation can be affected by colloids in natural waters [4,18,20–23], the term [Ox]/[Red] in
160 equation 1 should include colloid-bound species. This observation offers new perspectives to
161 explore unforeseen thermodynamic effects related to interfacial processes. Figure 1,
162 schematically depicts the adsorption and redox reactions of a TE's oxidized and reduced forms
163 (“Ox” and “Red”). The cartoon in Figure 1 showcases four Red and four Ox ions. The change in
164 Gibbs free energy in the oxidation reaction of the aqueous species Red to Ox (ΔG_{aq}) is in many
165 cases tabulated in thermodynamic databases, however, the free energy of the corresponding
166 reaction at the surface (ΔG_{surf}) will be different, because different species are involved (i.e.
167 aqueous species *versus* surface complexes), and is usually unknown. The relationship between
168 the two distinct redox reaction can be calculated if the Gibbs free energy of the respective
169 adsorption reactions of Ox ($\Delta G_{ads,Ox}$) and Red ($\Delta G_{ads,Red}$) are known:

$$170 \Delta G_{surf} = \Delta G_{aq} + \Delta G_{ads,Ox} - \Delta G_{ads,Red} \quad (4)$$

171
172 This relationship provides a quantitative measure for the difference between ΔG_{surf} and ΔG_{aq}
173 (as well as the corresponding $E_{Ox/Red}^0$ values in eq. 1), depending on the affinity of Ox and Red
174 for the surface. This situation very-likely applies to the vast majority of TEs, whose oxidation
175 state primarily dictate their chemical behavior, and thus, also their adsorption behavior. For
176 instance, actinides and Tc in their tetravalent state (U/Np/Pu/Tc(IV)) are known to bind much
177 more strongly with colloids than their oxidized forms (i.e. U(VI)/Np/Pu(V)/Tc(VII)), [4] as
178 illustrated for Np adsorption onto a clay (illite) in Figure 1b [32]. Note that irreversibility of
179 adsorption reactions, which can be attributed to additional reactions such as surface
180 precipitation or incorporation, and may lead to additional complications, will not be discussed
181 here to keep the focus of this article.

182
183 The thermodynamic parameters of the adsorption reactions of Ox and Red can be either
184 determined experimentally, e.g. by measuring the amount of adsorbed the TE under
185 sufficiently oxidizing or reducing conditions, respectively, or predicted by surface

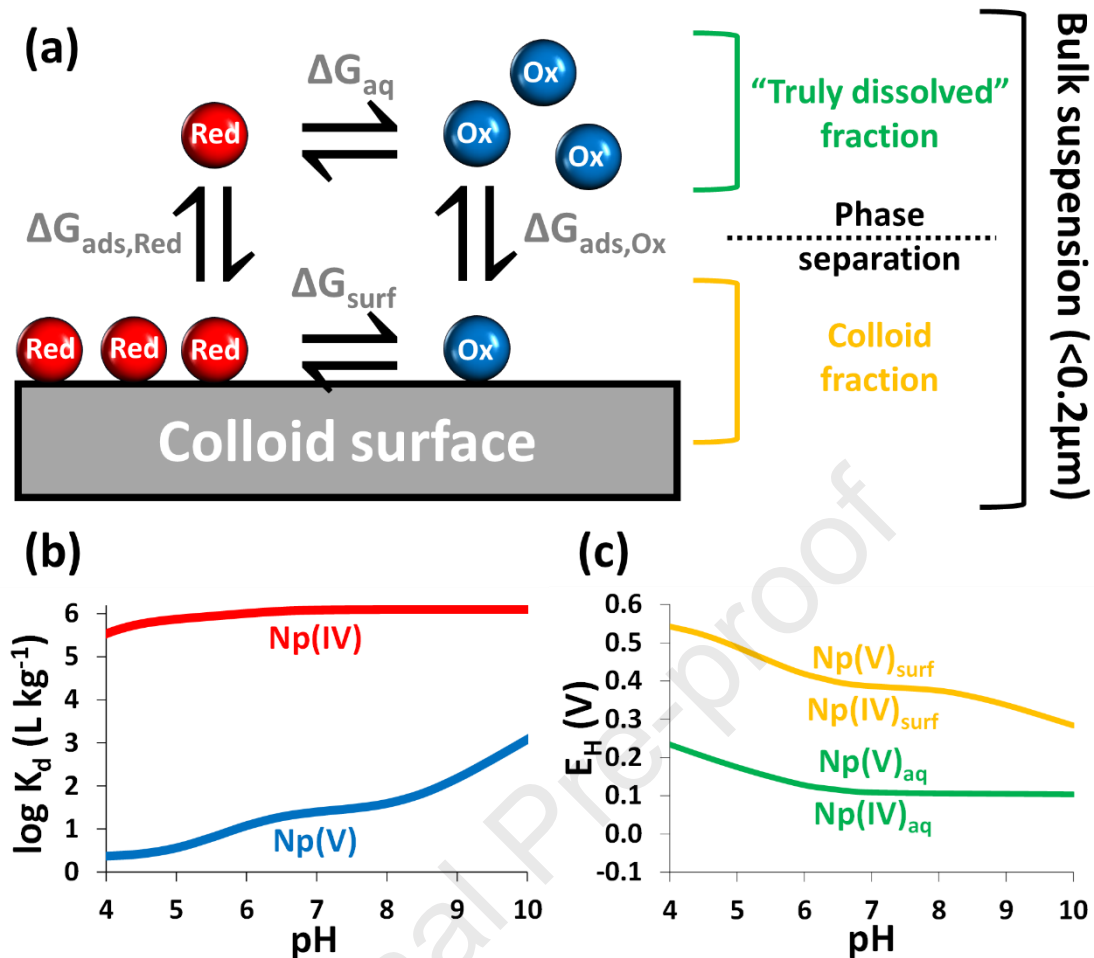
186 complexation models (SCM), provided that relevant parameters are available and
 187 trustworthy. For instance, missing SCM parameters associated with a redox-sensitive TE can
 188 be estimated by using relevant chemical analogues [4,33] or linear free energy relationships
 189 [47]. The choice of the SCM (e.g. with or without explicit description of electrostatic effects)
 190 has no real importance for the present calculations, provided that the model predictions are
 191 equal, which should in principle be the case when SCM are calibrated using the same
 192 experimental dataset. Experimental or model results can be provided as solid-liquid
 193 distribution coefficients (K_d , taken here in its unitless form):

$$194 \quad K_{d,Ox} = \frac{[Ox]_{surf}}{[Ox]_{aq}} \quad \text{and} \quad K_{d,Red} = \frac{[Red]_{surf}}{[Red]_{aq}} \quad (5)$$

196 which is a conditional thermodynamic parameter, describing adsorption phenomena in the
 197 specific physico-chemical conditions (surface loading, pH, ionic strength, T , etc.). Including it
 198 in equation 4 leads to the following equation:

$$200 \quad \frac{[Ox]_{aq}}{[Red]_{aq}} = \frac{[Ox]_{surf}}{[Red]_{surf}} \times \frac{K_{d,Red}}{K_{d,Ox}} \quad (6)$$

202 The consequences of equation 6 are illustrated in Figure 1, in which Red adsorbs more strongly
 203 to the surface ($K_{d,Red} = 3/1$) than Ox ($K_{d,Ox} = 1/3$). For an initially stoichiometric mixture of Ox
 204 and Red (4 ions each in total), adsorption processes imply that $[Ox]_{aq}/[Red]_{aq}$ is 9-fold larger
 205 than $[Ox]_{surf}/[Red]_{surf}$ (i.e. 3 *versus* 1/3). The above statements are further illustrated with
 206 modeling results in a more realistic system (Np-illite), for which the model was derived from
 207 batch experiments and spectroscopic investigations [32]. The adsorption of Np(IV) to illite is
 208 much larger than that of Np(V) (Figure 1b) whatever the pH. Therefore, the apparent redox
 209 potential of the Np(V)/Np(IV) couple in solution ($Np(V)_{aq}/Np(IV)_{aq}$) is lower than at the illite
 210 surface ($Np(V)_{surf}/Np(IV)_{surface}$). In other words, Np(V) is more easily reduced to Np(IV) at the
 211 illite surface. A comparison of the predominance pH- E_H ("Pourbaix") diagrams of Np in the
 212 aqueous phase or at the illite surface evidence an intermediate pH- E_H domain where Np(V)
 213 dominates in the aqueous phase whereas Np(IV) dominates at the illite surface (Figure 1c).
 214



215

216 **Figure 1.** (a) Cartoon of the adsorption and redox reactions involving the oxidized and the
 217 reduced forms of a TE (“Ox” and “Red”) in solution and at the surface of a colloid. Aqueous
 218 samples filtered at 0.2 μm are bulk colloid suspension that, upon further phase separation,
 219 split into so-called “truly dissolved” and colloid fractions. (b) Adsorption of Np(IV) (red) and
 220 Np(V) (blue) onto illite, quantified as solid-liquid distribution coefficients (K_d). (c)
 221 Predominance pH- E_H (“Pourbaix”) diagrams of Np either in the aqueous phase (green) or at
 222 the illite surface (orange). Modeling results in (b) and (c) where obtained for $[\text{Np}]_{\text{tot}} = 10^{-9}$ M,
 223 2 g L⁻¹ of illite in 0.1 M NaCl in reference [32].
 224

225 Field samples passed through a 0.2 or 0.45 μm filter, referred to as “bulk suspension” in
 226 Figure 1, do not provide data that can easily be interpreted by numerical modeling. Equations
 227 4 or 6 show the importance of colloids in the redox speciation calculations using the Nernst
 228 equation. Neglecting colloids, leads to erroneous conclusions because a mismatch between
 229 observation and calculation is inevitable. Solution analysis after further phase separation (e.g.
 230 by ultrafiltration, ultracentrifugation or some chromatographic techniques) might allow
 231 investigating the colloid-free, so-called “truly dissolved fraction” [19,21,22]. Such data should
 232 be better suited to the application of the Nernst equation, provided that (i) the original redox

233 state and speciation are maintained, and (ii) speciation of the TE in the truly dissolved fraction
234 can accurately be calculated or measured (i.e. in relation to equation 3). Therefore,
235 appropriate sample preparation and determination of the redox state distribution of the
236 element is required, and a consistent model must be adopted, i.e. accounting or not for the
237 colloid compartment depending on the sample filtration.

238

239 **3.2 Odd TE redox speciation explained by interfacial thermodynamics**

240 The above calculations are corroborated by the results of several studies dedicated to TE-
241 colloid interactions which have revealed the existence of an unforeseen oxidation state, that
242 can be explained by thermodynamic factors [26,32–38]. These results were obtained under
243 controlled laboratory conditions using purified colloids or synthetic materials that mimicked
244 natural colloids. This ensured that a steady-state was reached, that phase separation was
245 efficient and that geochemical speciation modeling may be accurate, thanks to the simplicity
246 of the system in relation to natural waters. Plutonium, with four oxidation states, ranging from
247 +III to +VI, and the capacity to disproportionate, as well as radiolytic processes induced by the
248 high activity of some of its isotopes, it is very easy to invoke any kind of kinetically controlled
249 process when thermodynamics appears to fail in predicting its complex chemistry. However,
250 several examples exist for which the Pu oxidation state distribution could be explained
251 accounting for the impact of colloids and surfaces:

- 252 • Pu(V) can be reduced to Pu(IV) at the surface of quartz in the presence of atmospheric O₂,
253 which is highly counter-intuitive but, in fact, this is due to the thermodynamic stability of
254 a Pu(IV) surface complex [35].
- 255 • Pu(V) reduction occurred in the presence of magnetite (Fe₃O₄) and mackinawite (FeS)
256 under anoxic conditions. Although the E_H values were similar in both cases, reduction only
257 proceeded to Pu(IV) where it precipitated as PuO_{2(s)} with mackinawite, because Pu has
258 weak affinity for surface S sites, whereas Pu(III) was found stabilized through surface
259 complexation on magnetite [37].
- 260 • Pu(III) oxidized to Pu(IV) at the surface of kaolinite and illite under reducing conditions.
261 Under oxidizing conditions, Pu(IV) prevailed on the surface of kaolinite but it partially
262 oxidized and prevailed as Pu(V) in the aqueous phase. These processes could be explained
263 using surface complexation modeling to account for the effects of adsorption on Pu redox

264 speciation under various physico-chemical conditions (e.g. pH, ionic strength, surface
265 loadings) [33,34].

266 As discussed above, similar observations were made for Ce, U and Np [32,36,38], which are
267 chemical analogues of Pu, with respect to their tetravalent oxidation state having a higher
268 affinity for the surface. Stabilization of one oxidation state with respect to others has not only
269 been observed not only for actinides but also for other TE such as Cu. It is expected to prevail
270 as Cu(II) and Cu(0) in oxidizing and reducing conditions, respectively, as Cu(I) is expected to
271 disproportionate. However, the presence of NOM can reduce the stability field of Cu(0) and
272 promote of the formation of Cu(I) complexes [26].

273

274 **4 Current challenges regarding the modelling of colloidal effects on the redox** 275 **speciation of trace elements in natural systems.**

276 **4.1 Redox potential determination**

277 All the approaches discussed above rely on the accurate determination of the E_H , which is a
278 considerable challenge to achieve. The simplest approach involves Pt-electrodes, but it cannot
279 be recommended due to the occurrence of several widely documented artifacts [6–8,45]. This
280 situation is likely discouraging for numerous scientists and, as other potential techniques are
281 more difficult to apply, in the vast majority of the studies focused on the redox speciation of
282 elements, no attempt is made to even measure an E_H value. However, there are also several
283 favorable outcomes, that should motivate hydro/bio/geochemists to attempt an E_H
284 measurement. In several studies, E_H measurements were corroborated by both independent
285 measurements and geochemical speciation modeling [13,32,48,49]. Recently [13,48], two
286 independent research teams measured consistently the E_H of 10 nm-sized magnetite
287 nanoparticles suspension, which provided key data for the understanding and the modeling
288 of the redox behavior of this highly reactive mineral. This is in line with the previous
289 demonstration that small iron oxide nanoparticles interact with the Pt-electrode, thus,
290 facilitating the E_H measurement [49]. Other electrodes can be efficient depending on the
291 studied system (e.g. using other metals such as Au-electrodes, or specifically designed
292 electrodes such as powder disk electrodes) [7,50], and electron mediators can be used to
293 facilitate the measurement [27]. The redox potential can also be determined indirectly by
294 performing redox state analysis of quinone-like compounds [28], or of a TE in the aqueous

295 phase and subsequent calculation using the Nernst equation, provided that phase separation
296 was efficient and the reaction database is complete enough to reach this aim [33]. Therefore,
297 the determination of the E_H is probably not impossible, but alternative methods have to be
298 developed, especially for the application in field studies [9]. Measurement by several
299 independent methods is encouraged to ensure reliable results, as the simple comparison
300 between E_H measurement with a Pt-electrode and calculations with the Nernst equation is
301 clearly not enough to do so.

302

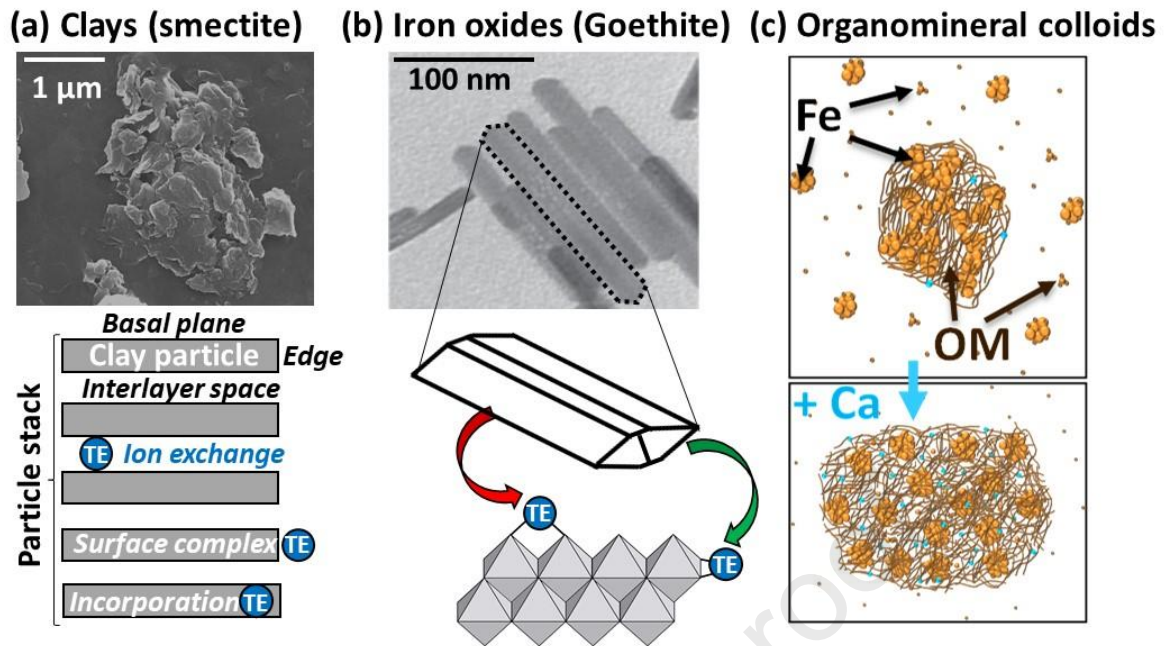
303 **4.2 The complex structure and heterogeneity of colloids, and the various related TE-** 304 **binding mechanisms**

305 The large heterogeneity and diversity of colloids is clearly an important bottleneck, limiting
306 the prediction of TE-colloid interactions in the environment. One of the common
307 characteristics of natural systems is the simultaneous presence of a wide variety of minerals
308 (such as Fe/Al/Mn (oxy)hydroxides, clays, etc.) and organic compounds (natural organic
309 matter (NOM): fresh biological compounds, humic substances, etc.), which can be released
310 into water bodies as colloids and may potentially be associated as heteroaggregates (e.g. Fig.
311 2a,b,c) [19,51,52]. Because TEs binding mechanisms mainly depend on the type of colloid, and
312 related TEs surface species formed, this requires to understand whether TEs (i) adsorb through
313 purely electrostatic attraction generated by either the variable surface charge or the
314 permanent charge of a mineral, (ii) form surface complexes with either organic or inorganic
315 moieties of colloids, (iii) incorporate into the bulk colloid structure or (iv) form precipitates
316 onto the colloid surface (see some examples in Fig. 2). Unfortunately, distinct mathematical
317 formalisms are required for each of these different processes, in order to simulate their impact
318 under various physico-chemical conditions encountered in natural systems (e.g., pH, ionic
319 strength, E_H , temperature). This issue is even more complex for redox-sensitive TEs, for which
320 the binding mechanisms must be elucidated for every oxidation state, as they behave as
321 distinct chemical elements. Great progresses are currently being made in predicting the ions
322 binding with nanoparticles and colloids, by accounting more accurately for interfacial
323 processes, surface site reactivity, and the information from the molecular to the aggregate
324 scale [53–56].

325 In natural colloidal heteroaggregates, composed of organomineral (e.g. Fe-oxides + NOM [51])
326 or inorganic assemblages (e.g. clays + Fe/Mn-oxides), each of the constitutive phases can

327 behave drastically differently from its individual counterparts. This is due to so-called “non-
328 additive” effects caused by the interactions between components, which requires further
329 experimental investigations and modelling development to be accurately taken into account
330 in surface speciation models [54,57,58]. Appropriate description of the surface speciation of
331 TEs might be required in order to identify the rate limiting reaction and to implement its rate
332 law expression in kinetic surface reaction modeling. If spectroscopic tools have widely been
333 used to determine the speciation of TEs in naturally heterogeneous samples, isotopic tools
334 have become very popular to probe interaction mechanisms between TEs and colloids. The
335 TEs isotopic fractionation can be driven by redox-dependent or independent processes
336 (adsorption). For instance, reduction of Cr(VI) to Cr(III) leads to significant isotopic
337 fractionation. During reactions, Cr isotopes fractionation happens because the Cr-O bonds
338 with light Cr isotopes are more easily broken compared to those of heavy isotopes, leading to
339 higher reaction rates of the lighter Cr isotope composition and consequent enrichment of
340 Cr(III) in the product [59]. But isotope fractionation at the mineral-water interface as also been
341 reported in the absence of redox processes or in the case of redox-inert TEs [60,61]. There is
342 still much to discover how TEs isotopes fractionate at the colloids-water interfaces as this tool
343 can be applied to various redox sensitive TEs. In addition, further experimental approaches
344 can take advantage of TE isotopes. Isotopic dilution techniques have been acknowledged as a
345 valuable tool for investigating various surface processes associated with the mobility of TEs
346 while determining the concentration of elements capable of isotopic exchange [62]. When
347 two compartments with distinct isotopic signatures (i.e. one natural and one artificially
348 modified) come into contact, isotopes tend to reach an equilibrium between solid and liquid
349 phases through isotopic exchange, without disturbance of the chemical equilibrium. Recent
350 studies specifically focused on the use of isotopic dilution to study the fate TEs in colloidal
351 suspension (e.g. [63]), while kinetic modelling of isotopic exchanges conducted to significant
352 scientific breakthrough in the understanding of additivity/non-additivity effects of TEs/bearing
353 phases interactions [64].

354



355

356 **Figure 2.** Examples of different constituents of colloids and binding mechanisms with TE: (a)
 357 clays (scanning electron microscopy image from [65]) and (b) iron oxides (transmission
 358 electron microscopy image from [66]) and some of the various possible interaction
 359 mechanisms with TEs. (c) Colloids structure is dynamic as illustrated here with a simple
 360 example: the impact of Ca^{2+} on the aggregation of organomineral colloids (illustration
 361 adapted from [51]).

362

363 4.3 Genesis and dynamics within the colloid compartment

364 Colloids are small particles that can easily change in size and shape due to, e.g.,
 365 recrystallization processes or aggregation phenomena (see e.g., Fig. 2c), or in composition due
 366 to matter transfer from or to the biota or soil/sediment compartments. Changes in the
 367 physical and chemical state of colloids inevitably affect TEs-colloid binding mechanisms and
 368 the driving forces of electron-transfer processes between TEs and colloids. Evolution of the
 369 colloid compartment occur, notably, through microbial activity being reductive or oxidative
 370 toward colloids, fluctuations or gradients of the E_H (e.g., in temporarily flooded soils such as,
 371 wetlands or coastal sediments), temperature (e.g., leading to ice melting in permafrost or to
 372 accepting or donating electron capacity changes), pH (e.g., in podzols or soils contaminated
 373 by mining activities) or salinity (e.g., in estuaries). Therefore, the concomitant evolution of the
 374 colloidal compartment and TEs redox speciation under the influence of
 375 bio/hydro/pedo/climatological constraints is a major obstacle to the understanding and
 376 prediction of related processes. It is necessary to comprehend the evolution of the colloidal

377 compartment in order to understand and predict its impact on TE redox speciation. This
378 concerns not only the redox potential and capacity (i.e. electron donating or accepting
379 capacity) of colloids [11–14], but also the binding capacity for TEs, as discussed above.
380 Due to their small size and high degree of heterogeneity, characterization of natural colloids
381 remains an important challenge, although great progress has been made during the past
382 years. For example, the use of ultrafiltration to separate the truly dissolved phase from the
383 colloidal phase, and to separate different ranges of colloidal sizes, has made it possible to
384 distinguish different behaviors with respect to trace elements [18,19,21,22]. To go further,
385 field flow fractionation (FFF) techniques combined with inductively coupled mass
386 spectrometry (ICP-MS) or time of flight ICP-MS used in single particle mode (spICP-ToF-MS)
387 coupled with machine learning algorithm [67–69], are particularly powerful techniques to
388 determine the size and composition of colloids, as well as to quantify the associated TEs.
389 Scanning transmission electron microscopy (STEM) with electron energy loss detection (EELS)
390 provides the atomic resolution suitable to identify traces of TEs at the surface of colloids, and
391 EELS spectra allow distinguishing not only elements but also their oxidation states [70].
392 However, if these tools allow investigating the heterogeneity within the colloid compartment,
393 new approaches are required to elucidate their dynamic behavior. Further developments of
394 *in situ* microscopic techniques, such as *in situ* STEM, would provide better understanding of
395 microbial effects on nanoparticle and colloid formation [71]. New *in situ* and *operando*
396 spectroscopic approaches inspired from the chemical catalysis community, might allow to
397 follow the transformation of colloids during wetting or drying of soils, and during the activity
398 of micro-organisms, by following the speciation of soil constituents with time. For instance,
399 oxidation processes of Fe(II) to Fe(III) by O₂ in the presence of NOM could be studied by Quick-
400 X ray absorption spectroscopy (XAS) [52]. Hyperspectral imaging adds spatial information to
401 time-resolved XAS data, which can be expected as highly valuable to investigate the formation
402 and transformation of colloids in soils [72]. Finally, isotopic tools could also probe the
403 formation and transformations of colloids, as it can be applied to elements like carbon,
404 nitrogen, sulfur, and other metals, as shown, for instance, in the case of natural Fe-NOM
405 heteroaggregates and complexes [73,74].

406 **5 Conclusions**

407 To predict the redox state distribution of TEs more accurately, new conceptual and numerical
408 models are needed. Over the past decades, the use of equilibrium thermodynamic models in
409 environmental studies has become less attractive because major elements (e.g.,
410 C/S/N/Fe/Mn/Al/Si) can react slowly in the environment and tend to form metastable phases,
411 including colloids. Recent scientific breakthroughs on the processes occurring at the interfaces
412 between water and nanoparticles/colloids may have provided important keys to the
413 appropriate use of thermodynamic models in a natural context. For example, they have been
414 shown to provide key insights for predicting the kinetically limited redox transformation of
415 organic pollutants. Equilibrium models accounting for TE adsorption processes on colloids also
416 provided robust interpretations of pH- and E_H -dependent TE redox speciation under
417 laboratory conditions. However, the colloidal compartment in field samples should be
418 analyzed more accurately, as 0.2 μ m filtration does not allow the concentration of truly
419 dissolved TEs and TEs bound to colloids to be distinguished, which would be of great help for
420 accurate geochemical speciation calculations. Further work is needed to accurately describe
421 and predict the binding of TEs to natural colloidal heteroaggregates, which will require the
422 development of advanced tools for field application as well as more mechanistic models of
423 the surface reactivity of these heterogeneous assemblages. Future models should decouple
424 the slow evolution of colloidal compartments in response to prevailing
425 bio/hydro/pedo/climatological conditions from the potentially faster redox transformation of
426 TEs occurring at the surface of colloids; an important key to a holistic understanding and
427 modeling of the fate and behavior of TEs in environmental systems.

428

429 **Acknowledgements**

430 This work was supported by the COLOSSAL project funded by ANR (project number ANR-23-
431 CE01-0001; coordinator: R. Marsac).

432

433 **Author contributions**

434 Rémi Marsac: Writing - original draft; Charlotte Catrouillet: Writing - review & editing; Mathieu
435 Pédrot: Writing - review & editing; Marc Benedetti: Writing - review & editing; Mélanie
436 Davranche: Writing - review & editing; Eric D. van Hullebusch: Writing - review & editing; Aline
437 Dia: Writing - review & editing; Yann Sivry: Writing - review & editing; Anne-Catherine Pierson-

438 Wickmann: Writing - review & editing; Mickael Tharaud: Writing - review & editing; Frank
439 Heberling: Writing - review & editing.

440

441 References

- 442 [1] Borch T, Kretzschmar R, Kappler A, Cappellen PV, Ginder-Vogel M, Voegelin A, et al.
443 Biogeochemical Redox Processes and their Impact on Contaminant Dynamics. *Environ Sci Technol*
444 2010;44:15–23. <https://doi.org/10.1021/es9026248>.
- 445 [2] Wang X, Wang W-X. Intracellular Biotransformation of Cu(II)/Cu(I) Explained High Cu Toxicity
446 to Phytoplankton *Chlamydomonas reinhardtii*. *Environ Sci Technol* 2021;55:14772–81.
447 <https://doi.org/10.1021/acs.est.1c05408>.
- 448 [3] Stumm W, Morgan JJ. *Aquatic Chemistry: Chemical Equilibria and Rates in Natural Waters*,
449 3rd ed. John Wiley&Sons, Inc., New York. 1996.
- 450 [4] Geckeis H, Lützenkirchen J, Polly R, Rabung T, Schmidt M. Mineral-water interface reactions
451 of actinides. *Chemical Reviews* 2013;113:1016–62. <https://doi.org/10.1021/cr300370h>.
- 452 [5] Altmaier M, Gaona X, Fanghänel T. Recent Advances in Aqueous Actinide Chemistry and
453 Thermodynamics. *Chem Rev* 2013;113:901–43. <https://doi.org/10.1021/cr300379w>.
- 454 [6] Lindberg RD, Runnells DD. Ground Water Redox Reactions: An Analysis of Equilibrium State
455 Applied to Eh Measurements and Geochemical Modeling. *Science* 1984;225:925–7.
456 <https://www.jstor.org/stable/1693951>.
- 457 [7] Sigg L. Redox Potential Measurements in Natural Waters: Significance, Concepts and
458 Problems. In: Schüring J, Schulz HD, Fischer WR, Böttcher J, Duijnsveld WHM, editors. *Redox:*
459 *Fundamentals, Processes and Applications*, Berlin, Heidelberg: Springer; 2000, p. 1–12.
460 https://doi.org/10.1007/978-3-662-04080-5_1.
- 461 [8] Wilkin R, Ludwig R, Ford R. Workshop on monitoring processes for groundwater restoration.
462 EPA Report 600/R-02/002; 2002.
- 463 [9] Peiffer S, Kappler A, Haderlein SB, Schmidt C, Byrne JM, Kleindienst S, et al. A
464 biogeochemical–hydrological framework for the role of redox-active compounds in aquatic systems.
465 *Nat Geosci* 2021;14:264–72. <https://doi.org/10.1038/s41561-021-00742-z>.
- 466 [10] Lacroix EM, Aeppli M, Boye K, Brodie E, Fendorf S, Keiluweit M, et al. Consider the Anoxic
467 Microsite: Acknowledging and Appreciating Spatiotemporal Redox Heterogeneity in Soils and
468 Sediments. *ACS Earth Space Chem* 2023;7:1592–609.
469 <https://doi.org/10.1021/acsearthspacechem.3c00032>.
- 470 [11] Klüpfel L, Piepenbrock A, Kappler A, Sander M. Humic substances as fully regenerable
471 electron acceptors in recurrently anoxic environments. *Nature Geosci* 2014;7:195–200.
472 <https://doi.org/10.1038/ngeo2084>.
- 473 [12] Gorski CA, Klüpfel L, Voegelin A, Sander M, Hofstetter TB. Redox Properties of Structural Fe in
474 Clay Minerals. 2. Electrochemical and Spectroscopic Characterization of Electron Transfer
475 Irreversibility in Ferruginous Smectite, SWa-1. *Environ Sci Technol* 2012;46:9369–77.
476 <https://doi.org/10.1021/es302014u>.

- 477 [13] Jungcharoen P, Pédrot M, Heberling F, Hanna K, Choueikani F, Catrouillet C, et al. Prediction
478 of nanomagnetite stoichiometry (Fe(II)/Fe(III)) under contrasting pH and redox conditions. *Environ*
479 *Sci: Nano* 2022;9:2363–71. <https://doi.org/10.1039/D2EN00112H>.
- 480 [14] Burgin AJ, Loecke TD. The biogeochemical redox paradox: how can we make a foundational
481 concept more predictive of biogeochemical state changes? *Biogeochemistry* 2023;164:349–70.
482 <https://doi.org/10.1007/s10533-023-01036-9>.
- 483 [15] Kleber M, Bourg IC, Coward EK, Hansel CM, Myneni SCB, Nunan N. Dynamic interactions at
484 the mineral–organic matter interface. *Nat Rev Earth Environ* 2021;2:402–21.
485 <https://doi.org/10.1038/s43017-021-00162-y>.
- 486 [16] Kappler A, Bryce C, Mansor M, Lueder U, Byrne JM, Swanner ED. An evolving view on
487 biogeochemical cycling of iron. *Nat Rev Microbiol* 2021;19:360–74. <https://doi.org/10.1038/s41579-020-00502-7>.
- 489 [17] Dong H, Zeng Q, Sheng Y, Chen C, Yu G, Kappler A. Coupled iron cycling and organic matter
490 transformation across redox interfaces. *Nat Rev Earth Environ* 2023;4:659–73.
491 <https://doi.org/10.1038/s43017-023-00470-5>.
- 492 [18] Kersting AB, Efurud DW, Finnegan DL, Rokop DJ, Smith DK, Thompson JL. Migration of
493 plutonium in ground water at the Nevada Test Site. *Nature* 1999;397:56–9.
494 <https://doi.org/10.1038/16231>.
- 495 [19] Allard T, Menguy N, Salomon J, Calligaro T, Weber T, Calas G, et al. Revealing forms of iron in
496 river-borne material from major tropical rivers of the Amazon Basin (Brazil). *Geochimica et*
497 *Cosmochimica Acta* 2004;68:3079–94. <https://doi.org/10.1016/j.gca.2004.01.014>.
- 498 [20] Ilina SM, Lapitskiy SA, Alekhin YV, Viers J, Benedetti M, Pokrovsky OS. Speciation, Size
499 Fractionation and Transport of Trace Elements in the Continuum Soil Water–Mire–Humic Lake–
500 River–Large Oligotrophic Lake of a Subarctic Watershed. *Aquat Geochem* 2016;22:65–95.
501 <https://doi.org/10.1007/s10498-015-9277-8>.
- 502 [21] Heydon M, Perez Serrano L, Schreck E, Causserand C, Pokrovsky OS, Behra P, et al. Role of
503 colloids in the transfer and dispersion of trace elements into river waters through a former mining
504 district. *Applied Geochemistry* 2023;155:105736.
505 <https://doi.org/10.1016/j.apgeochem.2023.105736>.
- 506 [22] Krickov IV, Lim AG, Vorobyev SN, Shevchenko VP, Pokrovsky OS. Colloidal associations of
507 major and trace elements in the snow pack across a 2800-km south-north gradient of western
508 Siberia. *Chemical Geology* 2022;610:121090. <https://doi.org/10.1016/j.chemgeo.2022.121090>.
- 509 [23] Pokrovsky OS, Dupré B, Schott J. Fe–Al–organic Colloids Control of Trace Elements in Peat Soil
510 Solutions: Results of Ultrafiltration and Dialysis. *Aquat Geochem* 2005;11:241–78.
511 <https://doi.org/10.1007/s10498-004-4765-2>.
- 512 [24] Elderfield H, Upstill-Goddard R, Sholkovitz ER. The rare earth elements in rivers, estuaries,
513 and coastal seas and their significance to the composition of ocean waters. *Geochimica et*
514 *Cosmochimica Acta* 1990;54:971–91. [https://doi.org/10.1016/0016-7037\(90\)90432-K](https://doi.org/10.1016/0016-7037(90)90432-K).
- 515 [25] Liger E, Charlet L, Van Cappellen P. Surface catalysis of uranium(VI) reduction by iron(II).
516 *Geochimica et Cosmochimica Acta* 1999;63:2939–55. [https://doi.org/10.1016/S0016-7037\(99\)00265-](https://doi.org/10.1016/S0016-7037(99)00265-3)
517 3.

518 [26] Maurer F, Christl I, Fulda B, Voegelin A, Kretzschmar R. Copper Redox Transformation and
519 Complexation by Reduced and Oxidized Soil Humic Acid. 2. Potentiometric Titrations and Dialysis Cell
520 Experiments. *Environ Sci Technol* 2013;47:10912–21. <https://doi.org/10.1021/es4024095>.

521

522 * [27] Chen G, Thompson A, Gorski CA. Disentangling the size-dependent redox reactivity of iron
523 oxides using thermodynamic relationships. *PNAS* 2022;119:e2204673119.
524 <https://doi.org/10.1073/pnas.2204673119>.

525 **The authors demonstrated a link between reduction potential values for the hematite/aqueous Fe²⁺**
526 **redox couple and the size of the particle, which explained the reduction rates of organic**
527 **contaminants.**

528

529 *[28] Aeppli M, Giroud S, Vranic S, Voegelin A, Hofstetter TB, Sander M. Thermodynamic controls
530 on rates of iron oxide reduction by extracellular electron shuttles. *PNAS* 2022;119:e2115629119.
531 <https://doi.org/10.1073/pnas.2115629119>.

532 **This article shows how free energy relationships aid in identifying controls on microbial iron oxide**
533 **reduction by extracellular electron shuttles, hence the role played by thermodynamics in important**
534 **biologically-mediated processes.**

535

536 [29] Wei H, Wang E. Nanomaterials with enzyme-like characteristics (nanozymes): next-
537 generation artificial enzymes. *Chem Soc Rev* 2013;42:6060–93. <https://doi.org/10.1039/C3CS35486E>.

538 [30] Gao L, Zhuang J, Nie L, Zhang Y, Gu N, et al. Intrinsic peroxidase-like activity of
539 ferromagnetic nanoparticles. *Nature Nanotech* 2007;2:577–83.
540 <https://doi.org/10.1038/nnano.2007.260>.

541 [31] Robinson TC, Latta DE, Notini L, Schilling KE, Scherer MM. Abiotic reduction of nitrite by
542 Fe(II): a comparison of rates and N₂O production. *Environ Sci: Processes Impacts* 2021;23:1531–41.
543 <https://doi.org/10.1039/D1EM00222H>.

544 [32] Banik NL, Marsac R, Lützenkirchen J, Marquardt CM, Dardenne K, Rothe J, et al. Neptunium
545 sorption and redox speciation at the illite surface under highly saline conditions. *Geochimica et*
546 *Cosmochimica Acta* 2017;215:421–31. <https://doi.org/10.1016/j.gca.2017.08.008>.

547 [33] Marsac R, Banik NL, Lützenkirchen J, Buda RA, Kratz JV, Marquardt CM. Modeling plutonium
548 sorption to kaolinite: Accounting for redox equilibria and the stability of surface species. *Chemical*
549 *Geology* 2015;400:1–10. <https://doi.org/10.1016/j.chemgeo.2015.02.006>.

550 [34] Marsac R, Banik NL, Lützenkirchen J, Diascorn A, Bender K, Marquardt CM, et al. Sorption and
551 redox speciation of plutonium at the illite surface under highly saline conditions. *Journal of Colloid*
552 *and Interface Science* 2017;485:59–64. <https://doi.org/10.1016/j.jcis.2016.09.013>.

553 [35] Hixon AE, Arai Y, Powell BA. Examination of the effect of alpha radiolysis on plutonium(V)
554 sorption to quartz using multiple plutonium isotopes. *Journal of Colloid and Interface Science*
555 2013;403:105–12. <https://doi.org/10.1016/j.jcis.2013.04.007>.

- 556 [36] Chakraborty S, Favre F, Banerjee D, Scheinost AC, Mullet M, Ehrhardt J-J, et al. U(VI) Sorption
557 and Reduction by Fe(II) Sorbed on Montmorillonite. *Environ Sci Technol* 2010;44:3779–85.
558 <https://doi.org/10.1021/es903493n>.
- 559 [37] Kirsch R, Fellhauer D, Altmaier M, Neck V, Rossberg A, Fanghänel T, et al. Oxidation state and
560 local structure of plutonium reacted with magnetite, mackinawite, and chukanovite. *Environmental*
561 *Science and Technology* 2011;45:7267–74. <https://doi.org/10.1021/es200645a>.
- 562 [38] Ratié G, Zhang K, Iqbal M, Vantelon D, Mahé F, Rivard C, et al. Driving forces of Ce(III)
563 oxidation to Ce(IV) onto goethite. *Chemical Geology* 2023;633:121547.
564 <https://doi.org/10.1016/j.chemgeo.2023.121547>.
- 565 [39] Navrotsky A. Energetics at the nanoscale: Impacts for geochemistry, the environment, and
566 materials. *MRS Bulletin* 2016;41:139–45. <https://doi.org/10.1557/mrs.2015.336>.
- 567 [40] Navrotsky A, Mazeina L, Majzlan J. Size-Driven Structural and Thermodynamic Complexity in
568 Iron Oxides. *Science* 2008;319:1635–8. <https://doi.org/10.1126/science.1148614>.
- 569 [41] Navrotsky A, Ma C, Lilova K, Birkner N. Nanophase Transition Metal Oxides Show Large
570 Thermodynamically Driven Shifts in Oxidation-Reduction Equilibria. *Science* 2010;330:199–201.
571 <https://doi.org/10.1126/science.1195875>.
- 572 [42] Aeppli M, Voegelin A, Gorski CA, Hofstetter TB, Sander M. Mediated Electrochemical
573 Reduction of Iron (Oxyhydr-)Oxides under Defined Thermodynamic Boundary Conditions. *Environ Sci*
574 *Technol* 2018;52:560–70. <https://doi.org/10.1021/acs.est.7b04411>.
- 575 [43] Parkhurst DL, Appelo CAJ. Description of input and examples for PHREEQC version 3: a
576 computer program for speciation, batch-reaction, one-dimensional transport, and inverse
577 geochemical calculations. vol. 6-A43. Reston, VA: U.S. Geological Survey; 2013.
578 <https://doi.org/10.3133/tm6A43>.
- 579 [44] Gustafsson JP. Visual MINTEQ Version 30 2005.
- 580 [45] Shi Z, Nurmi JT, Tratnyek PG. Effects of Nano Zero-Valent Iron on Oxidation–Reduction
581 Potential. *Environ Sci Technol* 2011;45:1586–92. <https://doi.org/10.1021/es103185t>.
- 582 [46] Neal C, Lofts S, Evans CD, Reynolds B, Tipping E, Neal M. Increasing Iron Concentrations in UK
583 Upland Waters. *Aquat Geochem* 2008;14:263–88. <https://doi.org/10.1007/s10498-008-9036-1>.
- 584 [47] Dzombak DA, Morel FMM. Surface Complexation Modeling: Hydrous Ferric Oxide. Wiley-
585 Interscience, New York; 1990.
- 586 [48] Robinson TC, Latta DE, Leddy J, Scherer MM. Redox Potentials of Magnetite Suspensions
587 under Reducing Conditions. *Environ Sci Technol* 2022;56:17454–61.
588 <https://doi.org/10.1021/acs.est.2c05196>.
- 589 [49] Silvester E, Charlet L, Tournassat C, Géhin A, Grenèche J-M, Liger E. Redox potential
590 measurements and Mössbauer spectrometry of FeII adsorbed onto FeIII (oxyhydr)oxides. *Geochimica*
591 *et Cosmochimica Acta* 2005;69:4801–15. <https://doi.org/10.1016/j.gca.2005.06.013>.
- 592 [50] Gorski CA, Nurmi JT, Tratnyek PG, Hofstetter TB, Scherer MM. Redox Behavior of Magnetite:
593 Implications for Contaminant Reduction. *Environ Sci Technol* 2010;44:55–60.
594 <https://doi.org/10.1021/es9016848>.

595 [51] Beauvois A, Vantelon D, Jestin J, Rivard C, Coz MB-L, Dupont A, et al. How does calcium drive
596 the structural organization of iron–organic matter aggregates? A multiscale investigation. *Environ Sci:*
597 *Nano* 2020;7:2833–49. <https://doi.org/10.1039/D0EN00412J>.

598 [52] Vantelon D, Davranche M, Marsac R, Fontaine CL, Guénet H, Jestin J, et al. Iron speciation in
599 iron–organic matter nanoaggregates: a kinetic approach coupling Quick-EXAFS and MCR-ALS
600 chemometrics. *Environ Sci: Nano* 2019;6:2641–51. <https://doi.org/10.1039/C9EN00210C>.

601 [53] Pinheiro JP, Rotureau E, Duval JFL. Addressing the electrostatic component of protons
602 binding to aquatic nanoparticles beyond the Non-Ideal Competitive Adsorption (NICA)-Donnan level:
603 Theory and application to analysis of proton titration data for humic matter. *Journal of Colloid and*
604 *Interface Science* 2021;583:642–51. <https://doi.org/10.1016/j.jcis.2020.09.059>.

605 [54] Gil-Díaz T, Jara-Heredia D, Heberling F, Lützenkirchen J, Link J, Sowoidnich T, et al. Charge
606 regulated solid-liquid interfaces interacting on the nanoscale: Benchmarking of a generalized
607 speciation code (SINFONIA). *Advances in Colloid and Interface Science* 2021;294:102469.
608 <https://doi.org/10.1016/j.cis.2021.102469>.

609

610 * [55] Liu L, Legg BA, Smith W, Anovitz LM, Zhang X, Harper R, et al. Predicting Outcomes of
611 Nanoparticle Attachment by Connecting Atomistic, Interfacial, Particle, and Aggregate Scales. *ACS*
612 *Nano* 2023;17:15556–67. <https://doi.org/10.1021/acsnano.3c02145>.

613 **The authors successfully applied an upscaling approach, from the atomic to the macroscopic scale,**
614 **to predict nanoparticle aggregation and attachment phenomena.**

615

616 [56] Boily J-F, Song X. Direct identification of reaction sites on ferrihydrite. *Commun Chem*
617 2020;3:1–8. <https://doi.org/10.1038/s42004-020-0325-y>.

618 [57] Reiller PE. Modelling metal–humic substances–surface systems: reasons for success, failure
619 and possible routes for peace of mind. *Mineralogical Magazine* 2012;76:2643–58.
620 <https://doi.org/10.1180/minmag.2012.076.7.02>.

621

622 * [58] Li J, Weng L, Deng Y, Ma J, Chen Y, Li Y. NOM-mineral interaction: Significance for
623 speciation of cations and anions. *Science of The Total Environment* 2022;820:153259.
624 <https://doi.org/10.1016/j.scitotenv.2022.153259>.

625 **This study provides explanation for some of the non-additive effects observed in the binding of**
626 **cations and anions to iron oxides-natural organic matter.**

627

628 [59] Schauble EA. Applying Stable Isotope Fractionation Theory to New Systems. *Reviews in*
629 *Mineralogy and Geochemistry* 2004;55:65–111. <https://doi.org/10.2138/gsrmg.55.1.65>.

630 [60] Frank AB, Klæbe RM, Frei R. Fractionation Behavior of Chromium Isotopes during the
631 Sorption of Cr (VI) on Kaolin and its Implications for Using Black Shales as a Paleoredox Archive.
632 *Geochemistry, Geophysics, Geosystems* 2019;20:2290–302. <https://doi.org/10.1029/2019GC008284>.

633

- 634 * [61] Yan X, Zhu M, Li W, Peacock CL, Ma J, Wen H, et al. Cadmium Isotope Fractionation during
635 Adsorption and Substitution with Iron (Oxyhydr)oxides. *Environ Sci Technol* 2021;55:11601–11.
636 <https://doi.org/10.1021/acs.est.0c06927>.
- 637 **In this article, Cd isotopes are used to probe the formation of different Cd species bound to iron**
638 **oxides. This one excellent example using such approach.**
- 639
- 640 [62] Collins RN, Tran ND, Bakkaus E, Avoscan L, Gouget B. Assessment of Isotope Exchange
641 Methodology to Determine the Sorption Coefficient and Isotopically Exchangeable Concentration of
642 Selenium in Soils and Sediments. *Environ Sci Technol* 2006;40:7778–83.
643 <https://doi.org/10.1021/es061528s>.
- 644 [63] Bolaños-Benítez V, van Hullebusch ED, Garnier J, Quantin C, Tharaud M, Lens PNL, et al.
645 Assessing chromium mobility in natural surface waters: Colloidal contribution to the isotopically
646 exchangeable pool of chromium (EwCr value). *Applied Geochemistry* 2018;92:19–29.
647 <https://doi.org/10.1016/j.apgeochem.2018.02.007>.
- 648 [64] Zelano IO, Sivry Y, Quantin C, Gélabert A, Maury A, Phalyvong K, et al. An Isotopic Exchange
649 Kinetic Model to Assess the Speciation of Metal Available Pool in Soil: The Case of Nickel. *Environ Sci*
650 *Technol* 2016;50:12848–56. <https://doi.org/10.1021/acs.est.6b02578>.
- 651 [65] Norrfors KK, Bouby M, Heck S, Finck N, Marsac R, Schäfer T, et al. Montmorillonite colloids: I.
652 Characterization and stability of dispersions with different size fractions. *Applied Clay Science*
653 2015;114:179–89. <https://doi.org/10.1016/j.clay.2015.05.028>.
- 654 [66] Xu J, Marsac R, Costa D, Cheng W, Wu F, Boily J-F, et al. Co-Binding of Pharmaceutical
655 Compounds at Mineral Surfaces: Molecular Investigations of Dimer Formation at Goethite/Water
656 Interfaces. *Environmental Science & Technology* 2017;51:8343–9.
657 <https://doi.org/10.1021/acs.est.7b02835>.
- 658 [67] Tharaud M, Schlatt L, Shaw P, Benedetti MF. Nanoparticle identification using single particle
659 ICP-ToF-MS acquisition coupled to cluster analysis. From engineered to natural nanoparticles. *J Anal*
660 *At Spectrom* 2022;37:2042–52. <https://doi.org/10.1039/D2JA00116K>.
- 661 [68] Meili-Borovinskaya O, Meier F, Drexel R, Baalousha M, Flamigni L, Hegetschweiler A, et al.
662 Analysis of complex particle mixtures by asymmetrical flow field-flow fractionation coupled to
663 inductively coupled plasma time-of-flight mass spectrometry. *Journal of Chromatography A*
664 2021;1641:461981. <https://doi.org/10.1016/j.chroma.2021.461981>.
- 665 [69] Ghotbizadeh M, Cuss CW, Grant-Weaver I, Markov A, Noernberg T, Ulrich A, et al.
666 Spatiotemporal variations of total and dissolved trace elements and their distributions amongst
667 major colloidal forms along and across the lower Athabasca River. *Journal of Hydrology: Regional*
668 *Studies* 2022;40:101029. <https://doi.org/10.1016/j.ejrh.2022.101029>.
- 669 [70] Hao X, Yoko A, Chen C, Inoue K, Saito M, Seong G, et al. Atomic-Scale Valence State
670 Distribution inside Ultrafine CeO₂ Nanocubes and Its Size Dependence. *Small* 2018;14:1802915.
671 <https://doi.org/10.1002/smll.201802915>.

672

- 673 * [71] Couasnon T, Alloyeau D, Ménez B, Guyot F, Ghigo J-M, Gélabert A. In situ monitoring of
674 exopolymer-dependent Mn mineralization on bacterial surfaces. *Science Advances*
675 2020;6:eaaz3125. <https://doi.org/10.1126/sciadv.aaz3125>.
- 676 **The authors used, for the first time, liquid-cell scanning transmission electron microscopy to observe**
677 **mineral growth on bacteria and the exopolymers they secrete.**
678
- 679 [72] La Fontaine C, Belin S, Barthe L, Roudenko O, Briois V. ROCK: A Beamline Tailored for
680 Catalysis and Energy-Related Materials from ms Time Resolution to μm Spatial Resolution.
681 *Synchrotron Radiation News* 2020;33:20–5. <https://doi.org/10.1080/08940886.2020.1701372>.
- 682 [73] Oleinikova OV, Poitrasson F, Drozdova OY, Shirokova LS, Lapitskiy SA, Pokrovsky OS. Iron
683 Isotope Fractionation during Bio- and Photodegradation of Organoferric Colloids in Boreal Humic
684 Waters. *Environ Sci Technol* 2019;53:11183–94. <https://doi.org/10.1021/acs.est.9b02797>.
- 685 [74] Lotfi-Kalahroodi E, Pierson-Wickmann A-C, Rouxel O, Marsac R, Bouhnik-Le Coz M, Hanna K,
686 et al. More than redox, biological organic ligands control iron isotope fractionation in the riparian
687 wetland. *Sci Rep* 2021;11:1933. <https://doi.org/10.1038/s41598-021-81494-z>.

Declaration of interests

The authors declare that they have no known competing financial interests or personal relationships that could have appeared to influence the work reported in this paper.

The authors declare the following financial interests/personal relationships which may be considered as potential competing interests:

Journal Pre-proof